BIOMOLECULES & THERAPEUTICS

Original Article
Biomol Ther 30(6), 585-592 (2022)

Hydroxyzine Induces Cell Death in Triple-Negative Breast Cancer Cells via Mitochondrial Superoxide and Modulation of Jak2/STAT3 Signaling

Rajina Shakya[1], Gyu Hwan Park[2], Sang Hoon Joo[1], Jung-Hyun Shim[3,*] and Joon-Seok Choi[1,*]

[1]*College of Pharmacy, Daegu Catholic University, Gyeongsan 38430,*
[2]*College of Pharmacy, Research Institute of Pharmaceutical Sciences, Kyungpook National University, Daegu 41566,*
[3]*College of Pharmacy, Mokpo National University, Muan 58554, Republic of Korea*

Abstract

Treatment of triple-negative breast cancer (TNBC) has been limited due to the lack of molecular targets. In this study, we evaluated the cytotoxicity of hydroxyzine, a histamine H1 receptor antagonist in human triple-negative breast cancer BT-20 and HCC-70 cells. Hydroxyzine inhibited the growth of cells in dose- and time-dependent manners. The annexin V/propidium iodide double staining assay showed that hydroxyzine induced apoptosis. The hydroxyzine-induced apoptosis was accompanied down-regulation of cyclins and CDKs, as well as the generation of reactive oxygen species (ROS) without cell cycle arrest. The effect of hydroxyzine on the induction of ROS and apoptosis on TNBC cells was prevented by pre-treatment with ROS scavengers, N-acetyl cysteine or Mito-TEMPO, a mitochondria-targeted antioxidant, indicating that an increase in the generation of ROS mediated the apoptosis induced by hydroxyzine. Western blot analysis showed that hydroxyzine-induced apoptosis was through down-regulation of the phosphorylation of JAK2 and STAT3 by hydroxyzine treatment. In addition, hydroxyzine induced the phosphorylation of JNK and p38 MAPK. Our results indicate that hydroxyzine induced apoptosis via mitochondrial superoxide generation and the suppression of JAK2/STAT3 signaling.

Key Words: Hydroxyzine, Reactive oxygen species, Triple-negative breast cancer, JAK2/STAT3, Cell cycle, Apoptosis

INTRODUCTION

Cancer remains to be the leading cause of death worldwide (Siegel *et al*., 2020). It can be initiated from the mutation in specific genes, and it is characterized by several features including constant cell proliferation, uncontrolled growth. Metastasis and the recurrence after anti-cancer therapy could be painful to the patients (Bertram, 2000; Gibbs, 2003). Even though attempts have been made to understand the complex mechanisms, complete remedy nor prevention has not been achieved yet (Baldwin, 2001).

Breast cancer is very common, and about two million women are diagnosed annually worldwide (Siegel *et al*., 2020). Common breast cancer treatment includes surgery, radiation, platinum chemotherapy, hormonal therapy, and more recent targeted therapy depending on the type and stage (Jacobs *et al*., 2022). Hormone receptors for estrogen and progesterone, and human epidermal growth factor 2 (HER2) can be good targets for anti-cancer therapy treating breast cancer. However, triple-negative breast cancer is characterized by the lack of hormone receptors and HER2, and does not respond to hormone antagonists or anti-HER2 monoclonal antibody (Cleator *et al*., 2007). Therefore, treatment of TNBC patients has been limited to standard chemotherapy. While recent advances with the development of targeted therapies, such as PARP inhibitor (Dent *et al*., 2013) and immune checkpoint inhibitor (Kwapisz, 2021), are noticeable, the development of molecular targets in treating TNBC would enhance the therapeutic impact.

Diverse biological processes including stem cell maintenance, development, inflammation, and hematopoiesis are modulated by the JAK2/STAT3 signaling pathway (Lopez-Onieva *et al*., 2008; Bollrath and Greten, 2009). STAT3 protein is often overexpressed in cancer cells (Bromberg *et al*., 1999) and regulates cell survival, apoptosis, and differentiation (Buettner

Open Access **https://doi.org/10.4062/biomolther.2022.121**

Received Sep 17, 2022 **Revised** Sep 30, 2022 **Accepted** Oct 1, 2022
Published Online Nov 1, 2022

***Corresponding Authors**
E-mail: joonschoi@cu.ac.kr (Choi JS), s1004jh@gmail.com (Shim JH)
Tel: +82-53-850-3611 (Choi JS), +82-61-450-2684 (Shim JH)
Fax: +82-53-359-6733 (Choi JS), +82-61-450-2689 (Shim JH)

et al., 2002). The activation of JAK/STAT signaling is related to the growth of cancer cells (Wang and Sun, 2014), whereas the inhibition, to the contrary, reduces the growth (Shan *et al*., 2010). Ruxolitinib is a kinase inhibitor selective to JAK1/2, and anti-cancer effect on TNBC has been studied (Stover *et al*., 2018). Similarly, L80, an HSP90 inhibitor, has been shown to suppress metastatic TNBC by inhibiting JAK2/STAT3 signaling axis (Cho *et al*., 2019). These suggest that JAK/STAT signaling might be one of the keys regulating the survival of TNBC cells.

Hydroxyzine, belonging to antihistamine drugs, has been used to treat itchiness, anxiety, and nausea for more than six decades (Bayart, 1956). It is a well-known histamine H1 receptor antagonist (Richelson, 1979), and safe enough to take the dosage of 100 mg (Smith *et al*., 2016). Interestingly, a couple of studies showed that histamine H1 receptor antagonists induced the apoptosis of tumor cells (Asuaje *et al*., 2018; Matsumoto *et al*., 2021). In addition, hydroxyzine was shown to inhibit the growth of cancer cell by decreasing the expression of translationally controlled tumor protein TCTP (Seo *et al*., 2017).

In this study, we investigated whether hydroxyzine could induce the apoptosis of human TNBC BT-20 and HCC-70 cells.

MATERIALS AND METHODS

Reagents

Hydroxyzine, Mito-TEMPO, and N-acetyl cysteine (NAC) were obtained from Sigma Aldrich (St. Louis, MO, USA). Primary antibodies against cleaved caspase-3, cleaved caspase-7, cleaved caspase-8, cleaved caspase-9, cleaved PARP, Bax, Bak, SOD1, cyclin D1, CDK2, STAT1, p-STAT1, STAT2, p-STAT3 (Ser727), p-STAT3 (Tyr705), JAK2, p-JAK2, Akt, p-Akt, ERK, p-ERK, JNK, p-JNK, p38, p-p38, HSP90, and c-Src were purchased from Cell Signaling Technology (Denver, CO, USA). Antibodies against Bcl-2, Bcl-xL, SOD2, cyclin A, cyclin D2, cyclin D3, cyclin E, p16, p21, p27, p53, p-JAK1, and MDM2 were obtained from Santa Cruz Biotechnology (Dallas, TX, USA). Also, anti-survivin antibody was purchased from Novus Biologicals (Centennial, CO, USA), and anti-beta-actin antibody was from Sigma Aldrich (Burlington, MA, USA). Anti-catalase and anti-cyclin B antibodies were obtained from Abcam (Cambridge, UK), and anti-JAK1 antibody was from Millipore (Burlington, MA, USA). All the horse-radish peroxidase (HRP)-conjugated secondary antibodies specific to mouse or rabbit antibody were purchased from Thermo Fisher Scientific (Waltham, MA, USA).

Cell lines and cell culture

The human breast cancer cell lines BT-20 and HCC-70 were from Korean Cell Line Bank (Seoul, Korea), and cultured in DMEM medium (Hyclone, Logan, UT, USA) supplemented with 10% fetal bovine serum (Hyclone) and 1% penicillin/streptomycin (Hyclone). The cells were incubated at 37°C in a 5% CO_2 humidified incubator. Unless stated otherwise, the effects of hydroxyzine on cancer cells were determined with varying concentration of hydroxyzine (0, 10, 20, and 50 μM) after incubating for 48 h. Dimethyl sulfoxide (Sigma Aldrich) was used as the vehicle.

WST (water-soluble tetrazolium) cell viability assay

Cell viability was assessed by water-soluble tetrazolium (WST) salt assay using the colorimetric QuantiMax™ WST assay reagent (BioMax, Seoul, Korea). First, BT-20 and HCC-70 cells were seeded at 1×10^4 cells per well in quadruplicate into a 48 well plate and grown for 24 h at 37°C in a 5% CO_2 incubator. The cells were then treated with 0, 5, 10, 20, 50, 75, and 100 μM of hydroxyzine. After 24 or 48 h treatment with hydroxyzine, the cells were incubated with QuantiMax™ WST reagent, and the absorbance was measured at 450 nm with a microplate reader (BMG Labtech, Ortenberg, Germany).

Annexin V/propidium iodide staining assay and cell cycle analysis

To detect the apoptosis of BT-20 and HCC-70 cells, Annexin V-fluorescein isothiocyanate apoptosis detection kit (BD Biosciences, San Diego, CA, USA) was used. Briefly, cells were harvested with trypsinization and washed twice with filtered 0.1% bovine serum albumin (BSA) in phosphate-buffered saline (PBS) and resuspended in 1x binding buffer containing Annexin V and propidium iodide (PI). Fluorescence intensity was measured by flow cytometry using a FACSCalibur flow cytometer (BD Biosciences).

For cell cycle analysis, the cells treated with hydroxyzine were washed with filtered 0.1% BSA in PBS and fixed in ice-cold 100% ethanol at 4°C overnight. The fixed cells were washed again with 0.1% BSA in PBS and stained with 50 μg/mL of propidium iodide (Life Technologies, Carlsbad, CA, USA) and 100 μg/mL of RNAase A (Biosesang, Daejeon, Korea) by incubating 30 min at room temperature. Fluorescence intensity was measured by flow cytometry to assess the DNA content.

Measurement of reactive oxygen species and mitochondrial membrane potential

To determine different indicators of reactive oxygen species, the cells treated with hydroxyzine were stained with specific indicators. The content of cellular reactive oxygen species was measured after staining the cells with 10 μM 2'7'-dichlorodihydrofluorescein diacetate (DCF-DA) (Life Technologies) for 1 h. 5 μM MitoSOX™ Red reagent (Thermo Fisher Scientific) was used to measure the mitochondrial superoxide contents, and 3,3'-dihexyloxacarbocyanine iodide ($DiOC_6$) (Life Technologies) was used to determine the mitochondrial membrane potential (MMP). Both mitochondrial superoxide contents and MMP were measured by flow cytometry after staining with indicators for 30 min at room temperature.

Western blot assay

The cells treated with hydroxyzine were harvested, washed with PBS, and lysed with RIPA buffer containing 1 mM sodium orthovanadate, 1 mM NaF, 0.1 mM phenylmethylsulfonyl fluoride, and a protease inhibitor cocktail. Pierce Coomassie (Bradford) protein Assay Kit (Thermo Fisher Scientific) was used to measure the protein yield following the manufacturer's instructions. Equal amounts of protein samples were resolved by 10% or 15% sodium dodecyl sulfate polyacrylamide gel electrophoresis. The resolved proteins were transferred to a polyvinylidene difluoride membrane (EMD Millipore Corporation, Billerica, MA, USA). The membrane was blocked with 5% skim milk in Tris-buffered saline-Tween® 20 detergent (TBST) for 1 h at room temperature, then washed with TBST briefly before the incubation with primary antibodies [1;1,000 dilution in 2% skim milk in TBST] overnight at 4°C. The membrane

incubated with the primary antibodies was washed with TBST and incubated with the secondary antibodies [1:5,000 dilution] for 2 h at room temperature. The proteins on the membrane were visualized by chemiluminescence using Amersham enhanced chemiluminescence (ECL) reagent (GE Lifesciences, Piscataway, NJ, USA).

Statistical analysis

Data are presented as the mean standard deviation. Single comparisons were performed using the Student's t-test. Data analysis was performed using SigmaStat 3.5 (Systat Software, Inc., San Jose, CA, USA). A probability (*p*) value less than 0.05 was considered statistically significant.

RESULTS

Hydroxyzine induced apoptosis in triple-negative breast cancer cell lines

We first investigated the effect of hydroxyzine on the viability of BT-20 and HCC-70 cells, triple-negative cancer cell lines, using a WST assay. Fig. 1A shows that hydroxyzine reduced cell viability in dose- (0, 5, 10, 20, 50, 75, and 100 μM) and time-dependent (24, and 48 h) manners significantly. The IC_{50} values of the inhibition of cell growth were 79.9 μM at 24 h and 45.4 μM at 48 h for BT-20 cells, and 64.6 μM at 24 h and 55.7 μM at 48 h for HCC-70 cells. We could notice the characteristic morphological changes, cell shrinkage and detachment of cells, of the cells treated with hydroxyzine (Fig. 1B). We then conducted annexin V/PI staining by flow cytometry. As the concentration of hydroxyzine increased from 0 to 10, 20, and 50 μM, the percentage of cells undergoing apoptosis increased from 12.8 to 18.6, 18.4, and 19.9%, respectively, for BT-20 cells. Likewise, the percentage of apoptotic HCC-70 cells increased from 13.9 to 14.5, 18.9, and 33.1% as the concentration of hydroxyzine increased from 0 to 10, 20, and 50 μM, respectively (Fig. 1C). Also, we investigated the activation of caspase cascade by hydroxyzine treatment. The western blot analysis showed that hydroxyzine treatment increased the levels of cleaved caspases, including caspase-3, -7, -8, as well as cleaved PARP, a substrate of caspase-3 (Fig. 1D), implying the activation of caspase cascade by hydroxyzine.

Hydroxyzine perturbed the balance of pro-apoptotic and anti-apoptotic Bcl-2 family proteins

To determine if hydroxyzine regulated the mitochondrial pathway, we measured the MMP as an indicator of functional mitochondrial activity. After treatment with hydroxyzine, we could notice the decrease in MMP by 41.8%% and 11.6% in BT-20 and HCC-70 cells, respectively (Fig. 2A). Then, we analyzed the protein expression levels of Bcl-2 family members by western blots. When BT-20 and HCC-70 cells were incubated

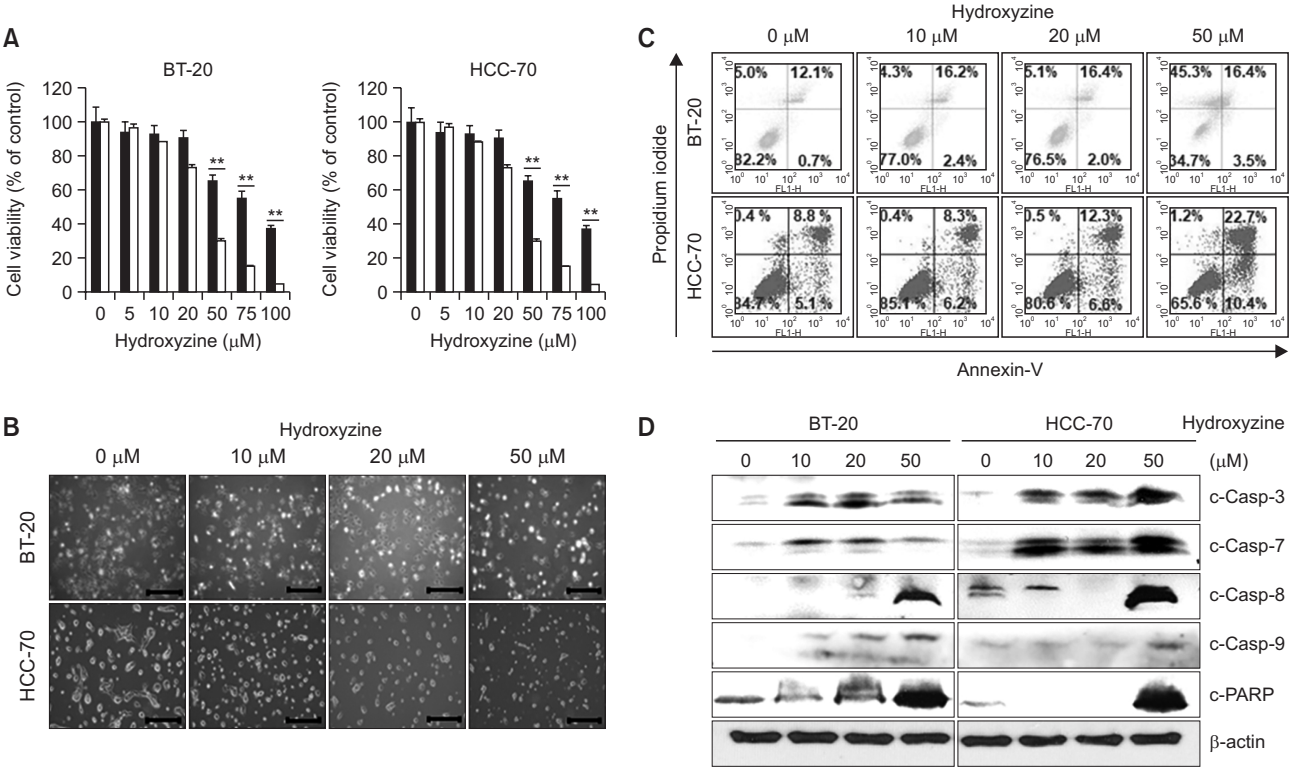

Fig. 1. Effect of hydroxyzine on cell proliferation and apoptosis. (A) Cells were treated with varying concentrations of hydroxyzine (0, 5, 10, 20, 50, 75, 100 μM) for 24, 48, or 72 h and cell viability was determined by WST assay. The data are expressed as the mean ± SD (n=4). ***p*<0.01 compared to the control group. (B) Morphological changes of TNBC cells after treatment with hydroxyzine for 24 h. Scale bar=200 μm. 100× magnification. (C) The cells treated with hydroxyzine were analyzed by flow cytometry using annexin V/PI stating. TNBC cells were treated with 0, 10, 20, and 50 μM of hydroxyzine for 48 h. Dot plots presenting the percentage of live (annexin V-/PI-, lower left), early apoptotic (annexin V+/PI-, lower right), late apoptotic (annexin V+/PI+, upper right), and necrotic (annexin V-/PI+, upper left) cells. (D) The levels of caspase-3, -7, -8, and -9, and cleaved PARP were analyzed by western blot. Actin was used as the loading control.

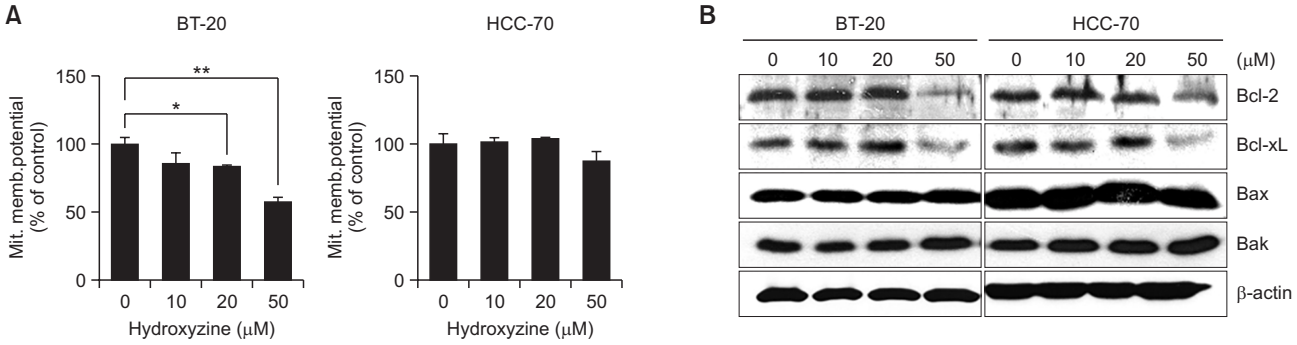

Fig. 2. Effect of hydroxyzine on Bcl-2 family proteins, caspases, and the mitochondrial membrane potential. TNBC cells were treated with hydroxyzine (0, 10, 20, and 50 μM) for 48 h. (A) The mitochondrial membrane potential was measured by flow cytometry after staining the cells with $DiOC_6$. The bar graphs represent the mean ± SD of triplicate determinations from three separate experiments. Statistical notations for differences in cell populations compared to controls: **p*<0.05 and ***p*<0.01. (B) The levels of Bcl-2 family proteins, Bcl-2, Bcl-xL, Bax, and Bak, were analyzed by western blot.

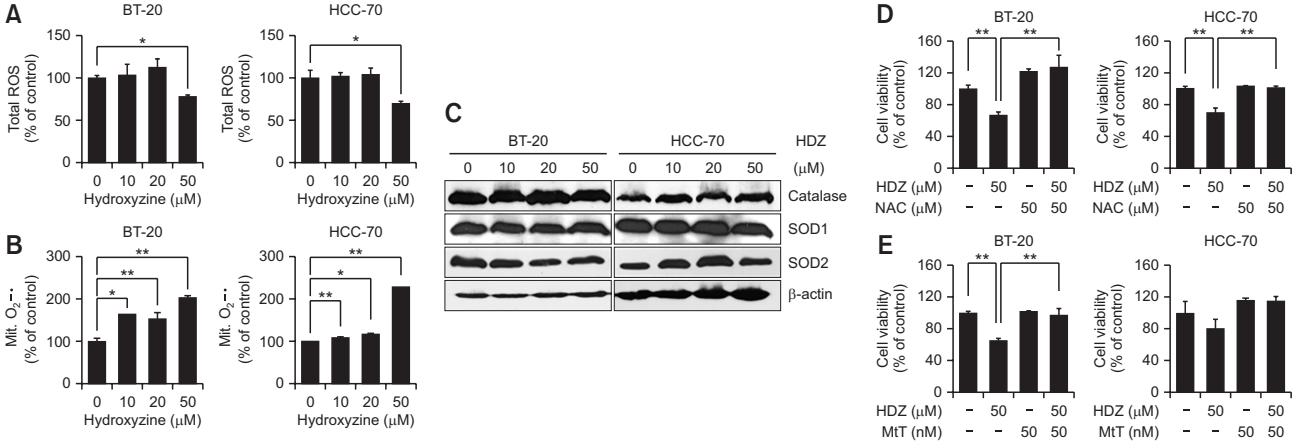

Fig. 3. Effect of hydroxyzine on the generation of ROS. TNBC cells were treated with hydroxyzine (0, 10, 20, and 50 μM) for 48 h. (A) The cellular level of ROS was measured by flow cytometry after staining the cells with DCF-DA. **p*<0.05. (B) The mitochondrial superoxide was measured by flow cytometry after staining the cells with MitoSOX™ Red. The bar graphs represent the mean ± SD of triplicate determinations from three separate experiments. Statistical notations for differences in cell cycle populations compared to controls: **p*<0.05, ***p*<0.01. (C) The levels of catalase, SOD1, and SOD were analyzed by western blot. (D, E) TNBC cells were pretreated with 50 μM of N-acetylcysteine (NAC) or 50 nM Mito-TEMPO for 3 h before hydroxyzine treatment for 48 h. The cell viability was measured by WST assay. ***p*<0.01 compared to controls.

with hydroxyzine, the levels of Bcl-2 and Bcl-xL decreased, whereas the levels of pro-apoptotic Bcl-2 family proteins, Bax and Bak, remained unchanged (Fig. 2B), indicating that the balance between pro-apoptotic and anti-apoptotic Bcl-2 family proteins was perturbed by hydroxyzine treatment. These results indicate that hydroxyzine activated the mitochondrial apoptotic pathway.

Hydroxyzine increased the generation of mitochondrial superoxide

The generation of excessive ROS can play a key role in apoptosis by different mechanisms (Ling *et al*., 2003; Richa *et al*., 2020). Therefore, we investigated if the generation of ROS was regulated by treatment of hydroxyzine. The level of cellular ROS was measured with DCF-DA staining, and we noticed that the level of cellular ROS decreased slightly by hydroxyzine treatment. Compared to the vehicle control, hydroxyzine at 50 μM decreased the total ROS by 30.2% and 21.2% in BT-20 and HCC-70 cells respectively (Fig. 3A). Interestingly, we noticed that hydroxyzine increased the mitochondrial superoxide level by 2.02 and 2.28-fold in BT-20 and HCC-70 cells respectively (Fig. 3B). The levels of proteins involved with the generation of reactive oxygen species, catalase, superoxide dismutase (SOD) 1 and SOD2, remained unchanged by hydroxyzine treatment (Fig. 3C). Next, we investigated if hydroxyzine-induced apoptosis could be prevented by scavenging ROS. The TNBC cells were pre-treated with 50 μM of N-acetylcysteine, an ROS scavenger, before hydroxyzine treatment. We could notice that hydroxyzine-induced cell death was prevented by 60 and 31.6% in BT-20 and HCC-70 cells respectively (Fig. 3D). Furthermore, pre-treatment with 50 nM Mito-TEMPO, a mitochondria-targeted antioxidant, resulted in the prevention of hydroxyzine-induced apoptosis by 30.8 and 25.9% in BT-20 and HCC-70 cells (Fig. 3E), implying the involvement of mitochondrial superoxide in hydroxyzine-induced apoptosis.

Hydroxyzine affects cell cycle regulatory proteins

To analyze whether the inhibition of cell proliferation induced by hydroxyzine was related to cell cycle arrest, we investigated the effect of hydroxyzine on the cell cycle phase populations of TNBC cells by flow cytometry. The percentage of BT-20 cells in the subG1 phase increased from 1.6% in the vehicle-treated group to 9% after treatment with 50 μM hydroxyzine. Similarly, and the percentage of HCC-70 cells in the subG1 phase increased from 2.6% to 11.8% by treatment of hydroxyzine at 50 μM. The percentage of cells in the subG1 phase converted to fold change compared to the control group was expressed as a graph (Fig. 4A, 4B). The assessment of protein levels of CDKs and cyclins indicated that CDK1, 2, and 4, cyclins A, B, and Ds decreased upon treatment with hydroxyzine, whereas the level of cyclin E alone increased (Fig. 4C). Interestingly, the level of CDK inhibitors, p16, p21, and p27 remained relatively constant upon hydroxyzine treatment (Fig. 4D).

Hydroxyzine suppressed the activation of JAK2/STAT3 signaling pathway

The JAK2/STAT3 signaling pathway controls the survival and proliferation of many cancer cells, and we examined the effects of hydroxyzine on JAK2 and STAT3 proteins by western blot analysis. Upon treatment with hydroxyzine, the level of JAK2 remained relatively constant in both BT-20 and HCC-70 cells. However, we noticed that the phosphorylation of JAK2 decreased in the higher concentration, 50 μM, of hydroxyzine. Furthermore, the protein level and phosphorylation status of STAT3 on serine 727 and tyrosine 705 were analyzed. The results showed that hydroxyzine reduced the levels of STAT3, p-STAT3 (Ser727), and p-STAT3 (Tyr705) in a dose-(0, 10, 20, and 50 μM) dependent manner (Fig. 5A).

Then we evaluated the protein level and phosphorylation status of protein kinases, Akt, ERK, JNK, and p38, which are related to cell survival. The change in either protein level or phosphorylation status of Akt and ERK was not noticeable upon treatment of hydroxyzine. However, we could see that the phosphorylation of both JNK and p38 was increased by hydroxyzine treatment, whereas the protein levels remained relatively unchanged (Fig. 5B).

DISCUSSION

Hydroxyzine is a piperazine derivative and exerts various actions such as antiemetic and sedative effects by working on central nervous system. While hydroxyzine is well-known histamine H1 receptor antagonist, it has also been shown to block dopamine receptor D2 (Haraguchi *et al*., 1997). The use

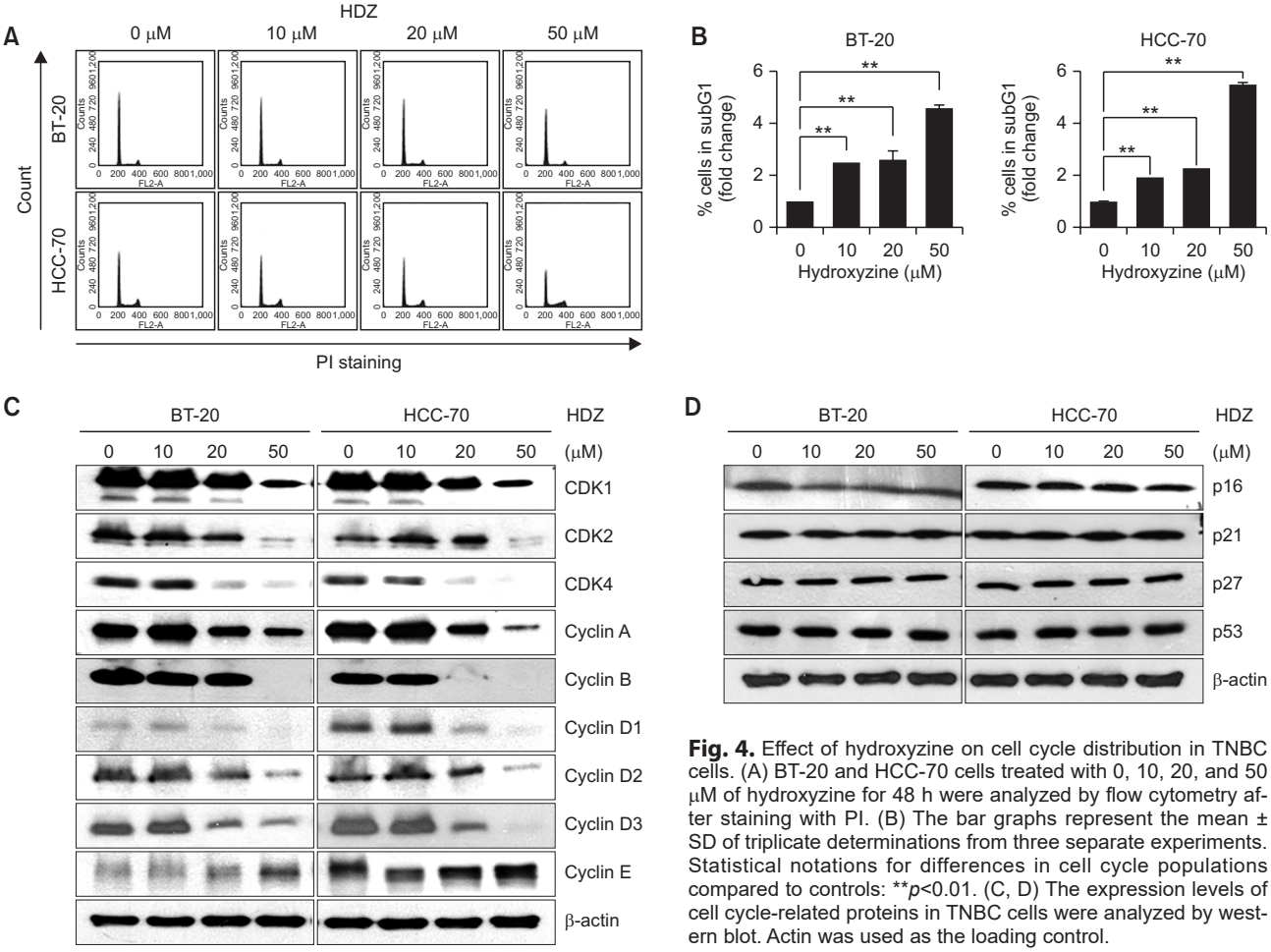

Fig. 4. Effect of hydroxyzine on cell cycle distribution in TNBC cells. (A) BT-20 and HCC-70 cells treated with 0, 10, 20, and 50 μM of hydroxyzine for 48 h were analyzed by flow cytometry after staining with PI. (B) The bar graphs represent the mean ± SD of triplicate determinations from three separate experiments. Statistical notations for differences in cell cycle populations compared to controls: $^{**}p<0.01$. (C, D) The expression levels of cell cycle-related proteins in TNBC cells were analyzed by western blot. Actin was used as the loading control.

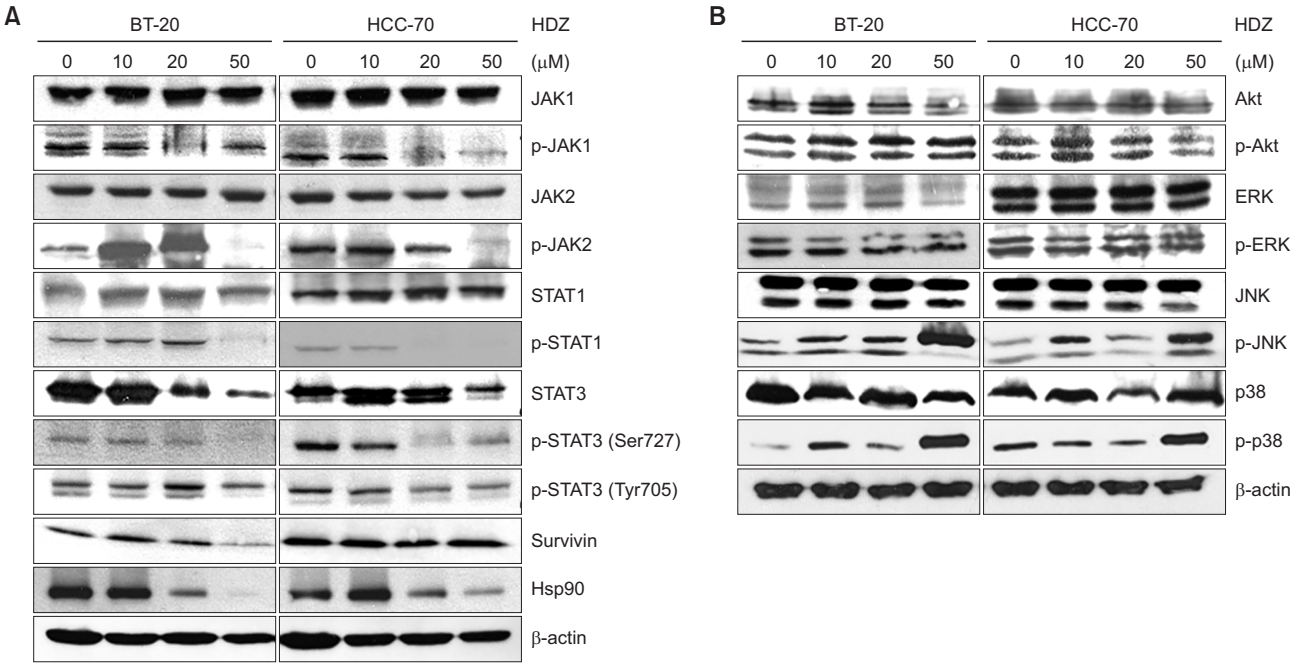

Fig. 5. Effect of hydroxyzine on Jak/STAT signaling. TNBC cells were treated with hydroxyzine (0, 10, 20, and 50 μM) for 48 h. (A) The levels of proteins involved in Jak/STAT signaling pathways were analyzed by western blot. (B) The levels of proteins involved in MAP kinase signaling pathways were analyzed by western blot. Actin was used as the loading control.

of hydroxyzine in cancer patients for sedative and antiemetic purposes has been well documented (Tsukuda *et al*., 1995), however, the anti-cancer effect of hydroxyzine has not been reported yet. This was the first report on the anti-cancer activity of hydroxyzine in human TNBC BT-20 and HCC-70 cells. Our cell viability assay results indicated that the proliferation of TNBC cells was inhibited by hydroxyzine in dose- and time-dependent manners.

Inducing apoptosis can be a good strategy of anticancer therapy (Lopez and Tait, 2015). Cancer cells can proliferate by either blocking the apoptotic pathway or activating the survival pathway (Wong, 2011). As we could see that hydroxyzine is cytotoxic to TNBC cells (Fig. 1A, 1B), we determined whether hydroxyzine induced apoptosis in TNBC cells. The results from annexin V apoptosis assay indicated that hydroxyzine treatment increased the rate of apoptosis significantly (Fig. 1C). The activation of caspases is involved with the progress of both intrinsic and extrinsic apoptotic pathways (McIlwain *et al*., 2013). As we attempted to delineate the molecular mechanism of hydroxyzine-induced apoptosis, we noticed the activation of caspases-3, -7, -8, and -9, as well as the cleavage of PARP (Fig. 1D). The activation of caspase-9, an initiator caspase in mitochondrial apoptotic signaling, indicated that hydroxyzine may induce apoptosis by activating the intrinsic pathway. The activation of caspases correlated well with the decrease in the mitochondrial membrane potential (Fig. 2A), and the shift in the balance of Bcl-2 family proteins as described below (Fig. 2B).

In addition to the caspase cascade, the generation of ROS was noticeable. Interestingly, we observed that the level of intracellular ROS in hydroxyzine-treated cells was slightly lower than that of untreated cells (Fig. 3A). Instead, we could see that mitochondrial superoxide was elevated in the TNBC cells treated with hydroxyzine (Fig. 3B). Meanwhile, the level of proteins possibly involved with the generation of ROS, catalase, SOD 1 and 2, remained relatively unchanged (Fig. 3C). Even though we observed the slight decrease in the cellular level of ROS in the TNBC cells treated with hydroxyzine, pretreatment of the cells with NAC at 50 μM, an inhibitor of ROS, prevented the apoptotic activity of hydroxyzine, indicating that the increased generation of ROS was involved with an upstream regulation of hydroxyzine-induced apoptosis (Fig. 3D). Moreover, the pretreatment of Mito-TEMPO, as little as 50 nM, showed the same level of prevention exerted by NAC at 50 μM (Fig. 3E). These results imply that the generation of mitochondrial superoxide was involved with the regulation of hydroxyzine-induced apoptosis.

To further study the detail of antiproliferative effect induced by hydroxyzine, we analyzed the cell cycle distribution in BT-20 and HCC-70 cells. We noticed the significant increase in the population of cells in subG1 phase (Fig. 4A), which implies that hydroxyzine induced apoptosis of TNBC cells. However, it appeared that the percentage of cells in each cell cycle phase remained relatively unchanged. The increase in the percentage of cells in subG1 phase correlated with the decrease in the levels of cyclins and CDKs except cyclin E (Fig. 4B). We speculate that hydroxyzine downregulated the cell cycle progress overall by lowering the levels of cyclins and CDKs. Notably, the percentage of S phase increased in the HCC-70 cells treated with hydroxyzine at 50 μM. It appears the increased level of cyclin E in HCC-70 cells resulted in the increase of cells in S phase (Chu *et al*., 2021). However, we doubt the increase in the percentage of S phase would contribute to the survival of HCC-70 cells, considering the lowered levels of other cyclins and CDKs. Contrary to the decreased the levels of cyclins and CDKs, the levels of p16, p21, and p27 did not

change by hydroxyzine treatment (Fig. 4C, 4D). This suggests that hydroxyzine-induced apoptosis was involved with overall downregulation of cyclins and CDKs rather than arresting cell cycle.

Modulation of several signaling pathways including PI3K/Akt, JAK2/STAT3, and MAPK/ERK affects the survival of cancer cells (Franceschelli *et al*., 2011; Wu *et al*., 2017). When the activation of JAK2/STAT3 signaling is not properly controlled, various types of cancer cells can proliferate (Nam *et al*., 2012; Yun *et al*., 2018). STAT3 protein is a transcription factor modulating various biological processes including proliferation, and cell differentiation, and apoptosis (Buettner *et al*., 2002; Park *et al*., 2021). The phosphorylation of STAT3 by JAK facilitates dimerization of STAT3. Then, STAT3 dimer moves into the nucleus and promotes the transcription of oncogenes. In this study, we determined the inhibitor effect of hydroxyzine on the JAK2/STAT3 signaling pathway in TNBC cells. As shown in Fig. 5A, we could notice that the levels of p-JAK2 and p-STAT3 were down-regulated significantly by hydroxyzine in a dose-dependent manner. In addition, hydroxyzine decreased the protein level of survivin in both BT-20 and HCC-70 cells. Next, we evaluated the level of expression and phosphorylation status of protein kinases involved with cell survival including Akt, ERK, JNK, and p38. The level of Akt and ERK, both in protein level and phosphorylation status, remained relative unchanged by hydroxyzine treatment (Fig. 5B). However, hydroxyzine increased the phosphorylation of stress-activated signaling molecules, JNK and p38 (Sui *et al*., 2014).

In conclusion, the results from this study demonstrate that hydroxyzine induced down-regulation of cyclins and CDKs, activation of mitochondrial apoptotic pathway, generation of mitochondrial superoxide, inactivation of STAT3-mediated signaling pathway, and activation of stress-activated signaling molecules JNK and p38. The further study would elucidate the molecular basis of hydroxyzine-induced cell death by revealing the molecular targets for treating TNBC cells.

CONFLICT OF INTEREST

The authors claim no conflicts of interest.

ACKNOWLEDGMENTS

This research was supported by Basic Science Research program through the National Research Foundation Korea Funded by the Ministry of Education, Science and Technology (NRF-2018R1D1A1A02050495 and NRF-2021R1A2C1014399).

REFERENCES

Asuaje, A., Martin, P., Enrique, N., Zegarra, L. A. D., Smaldini, P., Docena, G. and Milesi, V. (2018) Diphenhydramine inhibits voltage-gated proton channels (Hv1) and induces acidification in leukemic Jurkat T cells- new insights into the pro-apoptotic effects of antihistaminic drugs. *Channels (Austin)* **12**, 58-64.

Baldwin, A. S. (2001) Control of oncogenesis and cancer therapy resistance by the transcription factor NF-kappaB. *J. Clin. Invest.* **107**, 241-246.

Bayart, J. (1956) Treatment of nervousness in children with hydroxyzine. *Acta Paediatr. Belg.* **10**, 164-169.

Bertram, J. S. (2000) The molecular biology of cancer. *Mol. Aspects Med.* **21**, 167-223.

Bollrath, J. and Greten, F. R. (2009) IKK/NF-kappaB and STAT3 pathways: central signalling hubs in inflammation-mediated tumour promotion and metastasis. *EMBO Rep.* **10**, 1314-1319.

Bromberg, J. F., Wrzeszczynska, M. H., Devgan, G., Zhao, Y., Pestell, R. G., Albanese, C. and Darnell, J. E., Jr. (1999) Stat3 as an oncogene. *Cell* **98**, 295-303.

Buettner, R., Mora, L. B. and Jove, R. (2002) Activated STAT signaling in human tumors provides novel molecular targets for therapeutic intervention. *Clin. Cancer Res.* **8**, 945-954.

Cho, T. M., Kim, J. Y., Kim, Y. J., Sung, D., Oh, E., Jang, S., Farrand, L., Hoang, V. H., Nguyen, C. T., Ann, J., Lee, J. and Seo, J. H. (2019) C-terminal HSP90 inhibitor L80 elicits anti-metastatic effects in triple-negative breast cancer via STAT3 inhibition. *Cancer Lett.* **447**, 141-153.

Chu, C., Geng, Y., Zhou, Y. and Sicinski, P. (2021) Cyclin E in normal physiology and disease states. *Trends Cell Biol.* **31**, 732-746.

Cleator, S., Heller, W. and Coombes, R. C. (2007) Triple-negative breast cancer: therapeutic options. *Lancet Oncol.* **8**, 235-244.

Dent, R. A., Lindeman, G. J., Clemons, M., Wildiers, H., Chan, A., McCarthy, N. J., Singer, C. F., Lowe, E. S., Watkins, C. L. and Carmichael, J. (2013) Phase I trial of the oral PARP inhibitor olaparib in combination with paclitaxel for first- or second-line treatment of patients with metastatic triple-negative breast cancer. *Breast Cancer Res.* **15**, R88.

Franceschelli, S., Pesce, M., Vinciguerra, I., Ferrone, A., Riccioni, G., Patruno, A., Grilli, A., Felaco, M. and Speranza, L. (2011) Licocalchone-C extracted from Glycyrrhiza glabra inhibits lipopolysaccharide-interferon-gamma inflammation by improving antioxidant conditions and regulating inducible nitric oxide synthase expression. *Molecules* **16**, 5720-5734.

Gibbs, W. W. (2003) Untangling the roots of cancer. *Sci. Am.* **289**, 56-65.

Haraguchi, K., Ito, K., Kotaki, H., Sawada, Y. and Iga, T. (1997) Prediction of drug-induced catalepsy based on dopamine D1, D2, and muscarinic acetylcholine receptor occupancies. *Drug Metab. Dispos.* **25**, 675-684.

Jacobs, A. T., Martinez Castaneda-Cruz, D., Rose, M. M. and Connelly, L. (2022) Targeted therapy for breast cancer: an overview of drug classes and outcomes. *Biochem. Pharmacol.* **204**, 115209.

Kwapisz, D. (2021) Pembrolizumab and atezolizumab in triple-negative breast cancer. *Cancer Immunol. Immunother.* **70**, 607-617.

Ling, Y. H., Liebes, L., Zou, Y. and Perez-Soler, R. (2003) Reactive oxygen species generation and mitochondrial dysfunction in the apoptotic response to Bortezomib, a novel proteasome inhibitor, in human H460 non-small cell lung cancer cells. *J. Biol. Chem.* **278**, 33714-33723.

Lopez-Onieva, L., Fernandez-Minan, A. and Gonzalez-Reyes, A. (2008) Jak/Stat signalling in niche support cells regulates dpp transcription to control germline stem cell maintenance in the Drosophila ovary. *Development* **135**, 533-540.

Lopez, J. and Tait, S. W. (2015) Mitochondrial apoptosis: killing cancer using the enemy within. *Br. J. Cancer* **112**, 957-962.

Matsumoto, N., Ebihara, M., Oishi, S., Fujimoto, Y., Okada, T. and Imamura, T. (2021) Histamine H1 receptor antagonists selectively kill cisplatin-resistant human cancer cells. *Sci. Rep.* **11**, 1492.

McIlwain, D. R., Berger, T. and Mak, T. W. (2013) Caspase functions in cell death and disease. *Cold Spring Harb. Perspect. Biol.* **5**, a008656.

Nam, S., Xie, J., Perkins, A., Ma, Y., Yang, F., Wu, J., Wang, Y., Xu, R. Z., Huang, W., Horne, D. A. and Jove, R. (2012) Novel synthetic derivatives of the natural product berbamine inhibit Jak2/Stat3 signaling and induce apoptosis of human melanoma cells. *Mol. Oncol.* **6**, 484-493.

Park, B. K., Kim, D., Park, S., Maharjan, S., Kim, J., Choi, J. K., Akauliya, M., Lee, Y. and Kwon, H. J. (2021) Differential signaling and virus production in Calu-3 cells and Vero cells upon SARS-CoV-2 infection. *Biomol. Ther. (Seoul)* **29**, 273-281.

Richa, S., Dey, P., Park, C., Yang, J., Son, J. Y., Park, J. H., Lee, S. H., Ahn, M. Y., Kim, I. S., Moon, H. R. and Kim, H. S. (2020) A new histone deacetylase inhibitor, MHY4381, induces apoptosis via

generation of reactive oxygen species in human prostate cancer cells. *Biomol. Ther. (Seoul)* **28**, 184-194.
Richelson, E. (1979) Tricyclic antidepressants and histamine H1 receptors. *Mayo Clin. Proc.* **54**, 669-674.
Seo, E. J., Fischer, N. and Efferth, T. (2017) Role of TCTP for cellular differentiation and cancer therapy. *Results Probl. Cell Differ.* **64**, 263-281.
Shan, X. L., Zhou, X. Y., Yang, J., Wang, Y. L., Deng, Y. H. and Zhang, M. X. (2010) Inhibitory effect of cucurbitacin E on the proliferation of ovarian cancer cells and its mechanism. *Chin. J. Cancer* **29**, 20-24.
Siegel, R. L., Miller, K. D. and Jemal, A. (2020) Cancer statistics, 2020. *CA Cancer J. Clin.* **70**, 7-30.
Smith, E., Narang, P., Enja, M. and Lippmann, S. (2016) Pharmacotherapy for insomnia in primary care. *Prim. Care Companion. CNS Disord.* **18**, doi: 10.4088/PCC.16br01930.
Stover, D. G., Gil Del Alcazar, C. R., Brock, J., Guo, H., Overmoyer, B., Balko, J., Xu, Q., Bardia, A., Tolaney, S. M., Gelman, R., Lloyd, M., Wang, Y., Xu, Y., Michor, F., Wang, V., Winer, E. P., Polyak, K. and Lin, N. U. (2018) Phase II study of ruxolitinib, a selective JAK1/2 inhibitor, in patients with metastatic triple-negative breast cancer. *NPJ Breast Cancer* **4**, 10.
Sui, X., Kong, N., Ye, L., Han, W., Zhou, J., Zhang, Q., He, C. and Pan, H. (2014) p38 and JNK MAPK pathways control the balance of apoptosis and autophagy in response to chemotherapeutic agents. *Cancer Lett.* **344**, 174-179.
Tsukuda, M., Furukawa, S., Kokatsu, T., Enomoto, H., Kubota, A. and Furukawa, M. (1995) Comparison of granisetron alone and granisetron plus hydroxyzine hydrochloride for prophylactic treatment of emesis induced by cisplatin chemotherapy. *Eur. J. Cancer* **31A**, 1647-1649.
Wang, S. W. and Sun, Y. M. (2014) The IL-6/JAK/STAT3 pathway: potential therapeutic strategies in treating colorectal cancer (review). *Int. J. Oncol.* **44**, 1032-1040.
Wong, R. S. (2011) Apoptosis in cancer: from pathogenesis to treatment. *J. Exp. Clin. Cancer Res.* **30**, 87.
Wu, K. J., Huang, J. M., Zhong, H. J., Dong, Z. Z., Vellaisamy, K., Lu, J. J., Chen, X. P., Chiu, P., Kwong, D. W. J., Han, Q. B., Ma, D. L. and Leung, C. H. (2017) A natural product-like JAK2/STAT3 inhibitor induces apoptosis of malignant melanoma cells. *PLoS One* **12**, e0177123.
Yun, S., Yun, C. W., Lee, J. H., Kim, S. and Lee, S. H. (2018) Cripto enhances proliferation and survival of mesenchymal stem cells by up-regulating JAK2/STAT3 pathway in a GRP78-dependent manner. *Biomol. Ther. (Seoul)* **26**, 464-473.